scientific reports

Check for updates

OPEN

Epitope mapping of SARS-CoV-2 Spike protein using naturally-acquired immune responses to develop monoclonal antibodies

Rubén López-Aladid[1,2,11]✉, Leticia Bueno-Freire[1,2,11], Roc Farriol-Duran[3,4,11], Eduard Porta-Pardo[3,4], Ruth Aguilar[5], Marta Vidal[5], Alfons Jiménez[5,6], Roberto Cabrera[1,2], Nil Vázquez[1,2], Alexandre López-Gavín[1,2], Gemma Moncunill[5,7], Montserrat Carrascal[8], Teresa García[8], Miquel Lozano[9], Alberto L. García-Basteiro[5,6,7], Carlota Dobaño[5,7], Martalu D. Pazos[10], M.-Carmen Estevez[10], Laura M. Lechuga[10], Antoni Torres[1,2,12]✉ & Laia Fernández-Barat[1,2,12]✉

COVID-19 vaccination strategies are already available almost worldwide. However, it is also crucial to develop new therapeutic approaches, especially for vulnerable populations that may not fully respond to vaccination, such as the immunocompromised. In this project, we predicted 25 B-cell epitopes in silico in the SARS-CoV-2 Spike (S) protein and screened these against serum and plasma samples from 509 COVID-19 convalescent patients. The aim was to identify those epitopes with the highest IgG reactivity to produce monoclonal antibodies against them for COVID-19 treatment. We implemented Brewpitopes, a computational pipeline based on B-cell epitope prediction tools, such as BepiPred v2.0 and Discotope v2.0, and a series of antibody-epitope accessibility filters. We mapped the SARS-CoV-2 S protein epitopes most likely to be recognised by human neutralizing antibodies. Linear and structural epitope predictions were included and were further refined considering accessibility factors influencing their binding to antibodies like glycosylation status, localization in the viral membrane and accessibility on the 3D-surface of S. Blood samples were collected from 509 COVID-19 patients prospectively recruited 35 days after symptoms initiation, positive RT-qPCR or hospital/ICU discharge. Presence of IgG against SARS-CoV-2 was confirmed by lateral flow immunoassays. Epitopes immunogenicity was tested through the analysis of IgG levels and seropositivity in the convalescent serum and plasma samples and 126 pre-pandemic negative controls by Luminex to identify those with the highest reactivity. The seropositivity cut-offs for each epitope were calculated using a set of 126 pre-pandemic samples as negative controls (NC). Twenty-five SARS-CoV-2 S epitopes were predicted in silico as potentially the most immunogenic. These were synthesized and tested in a multiplex immunoassay against sera/plasmas from convalescent COVID-19 patients (5.7% asymptomatic, 35.6% mild, 13.8% moderate, 23% severe and 22% unknown because of anonymous donation). Among the 25 epitopes tested, 3 exhibited significantly higher IgG reactivity compared to the rest. The proportion of seropositive patients towards these 3 epitopes, based on median fluorescence intensity (MFI or Log_{10} MFI) above that from NC, ranged between 11 and 48%. Two out of the three most immunogenic epitopes were scaled up, resulting in the generation of two monoclonal antibodies (mAbs). These two mAbs exhibited comparable levels of S protein affinity to commercialized mAbs. Our data shows that the candidate S epitopes predicted in silico are recognised by IgG present in convalescent serum and plasma. This evidence suggests that our computational and experimental pipeline is able to yield immunogenic epitopes against SARS-CoV-2 S. These epitopes are suitable for the development of novel antibodies for preventive or therapeutic approaches against COVID-19.

Keywords Antibody, Immunoassay, Serology, SARS-CoV-2, Recovered patients of COVID-19, IgG, Luminex, Epitope mapping, Multiplex, Spike protein, Predictive models

[1]Cellex Laboratory, Centro de Investigación Biomédica en Red de Enfermedades Respiratorias (CIBERES, 06/06/0028), Fundació de Recerca Clínic Barcelona-Institut d'Investigacions Biomèdiques August Pi i Sunyer (FRCB-

IDIBAPS), School of Medicine, Universitat de Barcelona, Barcelona, Spain. [2]Pulmonology Service, Hospital Clínic de Barcelona, Barcelona, Spain. [3]Cancer Immunogenomics Institut Josep Carreras, Barcelona, Spain. [4]Barcelona Supercomputing Center (BSC), Barcelona, Spain. [5]ISGlobal, Barcelona, Spain. [6]Spanish Consortium for Research in Epidemiology and Public Health (CIBERESP), Barcelona, Spain. [7]Centro de Investigación Biomédica en Red de Enfermedades Infecciosas (CIBERINFEC), Barcelona, Spain. [8]Biological and Environmental Proteomics Group, Institute of Biomedical Research of Barcelona, Spanish National Research Council (IIBB-CSIC/IDIBAPS), Barcelona, Spain. [9]Institut Clínic del Càncer i Malalties de la Sang, Hospital Clínic, Institut d'Investigacions Biomèdiques August Pi i Sunyer (FRCB-IDIBAPS), Universitat de Barcelona ES, Barcelona, Spain. [10]Nanobiosensors and Bioanalytical Applications Group (NanoB2A), Catalan Institute of Nanoscience and Nanotechnology (ICN2), CSIC, BIST, CIBER-BBN, Bellaterra, Barcelona, Spain. [11]López-Aladid Rubén, Bueno-Freire Leticia and Farriol-Duran Roc contributed equally to this work. [12]These authors jointly supervised this work: Torres Antoni and Fernández-Barat Laia. ✉email: ruben.aladid@gmail.com; atorres@recerca.clinic.cat; lfernan1@recerca.clinic.cat

The severe acute respiratory syndrome coronavirus 2 (SARS-CoV-2) is responsible for the global pandemic of coronavirus disease 2019 (COVID-19)[1]. The Spike (S) protein on the virus surface plays a crucial role in mediating viral entry into host cells, making it an attractive target for developing monoclonal antibodies (mAbs) for therapeutic and diagnostic purposes. Epitope mapping of the S protein can identify regions that elicit neutralizing mAbs with potential therapeutic efficacy. To date, these regions have been predominantly described to target the receptor-binding domain (RBD) of the S1 fragment, critical for host cell invasion[2–4].

Several studies have utilized structural biology and bioinformatics to identify potent neutralizing mAbs[2–4]. Epitope mapping can provide insights into virus evolution and the protective immune response of infected and vaccinated individuals. For instance, some studies have identified S epitopes with mutations potentially affecting mAb efficacy targeting those regions[5,6]. Andreano et al. (2020) and Li et al. (2021) identified S epitopes targeted by the human immune response, shedding light on naturally acquired immunity to SARS-CoV-2[7,8]. These studies confirm previous findings and reveal new insights into different antibody isotypes and epitopes constituting the symptomatic signature of COVID-19 disease and RBD neutralizing regions of B cells.

In our research project, we utilized Brewpitopes, an in-house bioinformatic pipeline that refines bioinformatic B-cell epitope predictions to enhance their capacity to elicit neutralizing humoral responses[9]. This pipeline integrates three distinct software tools—ABCpred, Discotope v2.0, and BepiPred v2.0—to predict potential epitopes within the SARS-CoV-2 S protein[10–12]. Together, Discotope v2.0 and BepiPred v2.0 offer complementary approaches for epitope prediction, covering both conformational and linear aspects, thereby essential for comprehensive antigenic characterization and vaccine design. These tools include predictions of linear and structural epitopes, which are then prioritized according to multiple variables that influence the interaction between antibodies and their epitopes: glycosylation status, localization on the viral membrane and accessibility in the 3D conformation of their parental protein[11,12].

The aim of our study was to predict the most immunogenic SARS-CoV-2 S epitopes through computational analysis and screen their immunogenicity against plasma from COVID-19 convalescent patients to identify those that exhibited the strongest IgG reactivity as potential targets for mAb development. Secondly, we aimed to produce monoclonal antibodies recognizing our selected epitopes and finally to determine their affinity towards SARS-CoV-2 S protein.

Materials and methods

Study population and samples

COVID-19 recovered patients ($n = 397$) were prospectively recruited at the pulmonology service of Hospital Clínic de Barcelona (Spain) between April and December 2020. Inclusion criteria were as follows: (1) adults aged ≥ 18 and ≤ 90 years; (2) confirmed or suspected SARS-CoV-2 infection; (3) approximately 35 ± 5 days since symptom onset, positive RT-qPCR, or hospital discharge; (4) ability to perform all the clinical tests and understand the study's process and purposes; and (5) signed written informed consent. The exclusion criteria applied were: (1) immunocompromised state or chronic immunosuppressive medication; (2) untreated or uncontrolled chronic viral infection (e.g. HIV, HBV, HCV); (3) malignancy requiring active treatment within the past three months; and (4) any physical or psychological disorder that might interfere with protocol compliance. Additionally, 39 serum samples were obtained from the Blood and Tissue Bank (BTB) in Barcelona from anonymous donors, and 73 plasmas were collected by ISGlobal from SARS-CoV-2 IgG-positive healthcare workers, resulting in a total sample size of 509 participants (Fig. 1). The demographics of the anonymous donors were not available.

The study was approved by the Clinical Research Ethics Committee of the Hospital Clínic de Barcelona (Ethics Approval Reference: HCB/2020/0332) and was conducted in accordance with applicable legislation (Spanish Biomedical Research Law 14/2007). Written informed consent was obtained from all study participants. Samples were anonymized with a successive numerical code that can only be related to the clinical history by the study investigators. Demographics of the anonymous patients ($n = 112$) were not available.

For patients attending Hospital Clínic, a single visit was conducted to: (1) record socio-demographic and clinical data, (2) collect finger-prick blood samples, and (3) confirm IgG and/or IgM seropositivity against SARS-CoV-2. Socio-demographic and clinical data included: age, sex, date of symptom onset and diagnosis, diagnostic method and result, symptoms (malaise, fever, cough, myalgia, anosmia, ageusia, headache, gastrointestinal symptoms, dyspnoea, others), presence of co-infection, hospitalization and length of stay, oxygen therapy, intensive care unit (ICU) admission and length of ICU stay, days under mechanical ventilation, treatment, and complications (acute respiratory distress syndrome [ARDS], bilateral pneumonia, organizing pneumonia, coagulopathy, others). Patients were classified into four groups depending on COVID-19 severity: (1) asymptomatic (absence of symptoms during infection), (2) mild (presence of mild clinical signs or symptoms only requiring symptomatic treatment), (3) moderate (concomitant medication [other than symptomatic] was

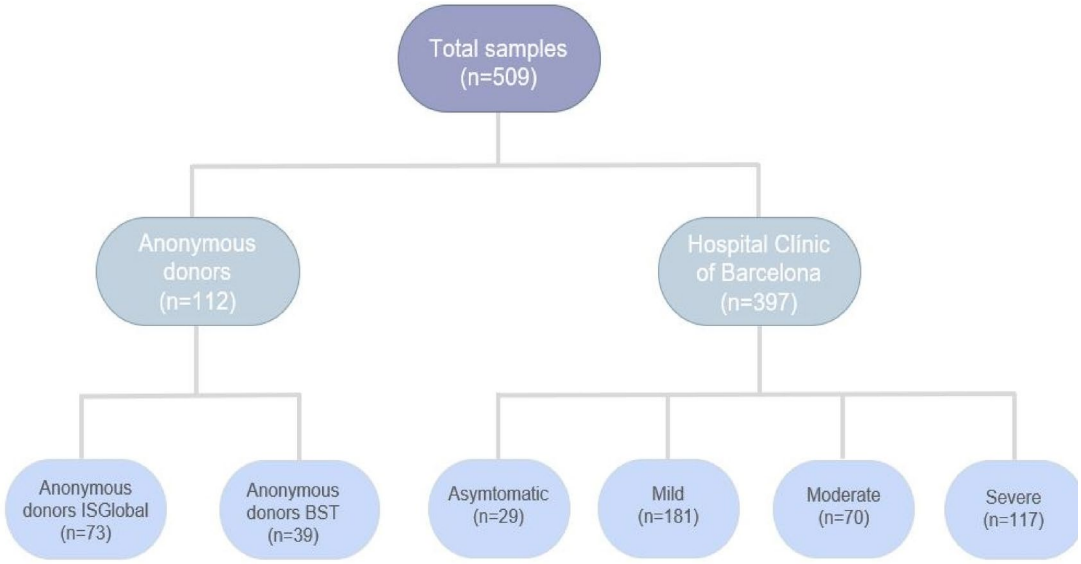

Fig. 1. Study samples flow-chart.

added, and/or oxygen therapy requirement, and/or hospital admission), and (4) severe (intermediate care unit or ICU admission, and/or high flow oxygen, and/or mechanical ventilation requirements).

Lateral flow immunoassay classification

Finger-prick blood samples were used to confirm seropositivity against SARS-CoV-2 using lateral flow immunoassays (Abingdon Health, York, UK). The results were classified into four groups: (1) negative, (2) IgM positive, (3) IgM and IgG positive, and (4) IgG positive. IgG results were further categorized into (A) weak positive (IgG+), (B) positive (IgG++), and (C) strong positive (IgG+++). This classification was performed visually by a single, trained researcher to ensure consistency across the samples. The results were cross-validated by multiple trained individuals to minimize subjectivity and ensure reliability of the visual inspection.

Additionally, blood samples were subsequently processed and stored at -80ºC at IDIBAPS Biobank until Luminex immunoassays.

Computational pipeline to refine bioinformatic B-cell epitope predictions

We implemented Brewpitopes[9], a computational pipeline to refine B-cell epitope predictions from linear predictors (BepiPred v2.0[12] and ABCpred[10]) and for conformational tools (Discotope v2.0[11]) on the S protein and predict the epitopes most likely to be recognised by neutralising antibodies. Our pipeline integrated predictions of linear and structural epitopes into consensus epitope regions using the in-house Epixtractor and Epiconsensus modules[9]. Then, these candidates were prioritized based on multiple factors influencing the surface accessibility of the epitopes and exposition to neutralizing antibodies. These consisted of the localization on the viral membrane or extra virality, which was predicted using CCTOP[13] and the Epitopology module; the absence of glycosylated residues in the epitope sequence, predicted using Net-N-Glyc[14], Net-O-Glyc[15] and Epiglycan[9]; and the surface accessibility in the 3D conformation of their parental protein, which was predicted using the Episurf module to calculate the residue solvent accessibility (RSA) of the epitope residues[9]. Residues with higher RSA than 0.2 were considered exposed. Additionally, predicted peptides shorter than 6AA were removed due to lack of sequence specificity. All this pipeline has been streamlined to enhance its throughput to facilitate proteome-wide predictions - as described for the SARS-CoV-2-proteome in our previous study[9].

Conservation of epitope candidates across SARS-CoV-2 variants was evaluated using a complementary in silico analysis. Amino acid mutations corresponding to the main SARS-CoV-2 Variants of Concern (VOCs) — Alpha, Beta, Gamma, Delta, and Omicron — were retrieved from the CoVariants server (https://covariants.org), which is powered by GISAID. Using these data, we reconstructed variant-specific S protein sequences by introducing the corresponding mutations into the ancestral sequence via an in-house R script (fasta_mutator.R), as previously described[9]. Our candidate peptides were then mapped onto these sequences to assess their conservation across variants. This step was incorporated to prioritize epitope regions that are resilient to viral antigenic drift and potentially suitable for broad-spectrum antibody targeting.

Peptide synthesis

Peptide epitopes (peptides) were synthetized by BCN Peptides (BCN Peptides, Spain). During the process, amino acids were obtained as protected derivatives to prevent unwanted reactions. Solvents such as dimethyl sulfoxide (DMSO) and methanol were utilized to dissolve reagents and establish the necessary reaction environment. Coupling reagents like DIC and HOBt facilitated bond formation between amino acids. Temporary blocking of specific functional groups on amino acids was achieved using protecting groups like Fmoc and Boc to prevent undesired reactions. Peptides were typically synthesized via solid-phase synthesis, wherein the initial amino acid

was attached to a solid support, and subsequent amino acids were sequentially added to construct the peptide chain. Activation and coupling occurred by activating amino acid residues with a coupling reagent and coupling them to the growing peptide chain on the solid support. Once the desired peptide sequence was assembled, protecting groups were removed to expose functional groups. Subsequently, the peptide was cleaved from the solid support using a cleavage reagent such as trifluoroacetic (TFA). The crude peptide mixture underwent purification techniques such as chromatography to yield a highly pure peptide. Finally, the synthesized peptide was characterized using methods like high-performance liquid chromatography (HPLC) and mass spectrometry to confirm its identity and purity.

Antigen epitope mapping by luminex

Plate format and sample processing

Each Luminex assay plate used 384-well plates to allow for high-throughput processing. Each plate included 126 pre-pandemic plasma samples to determine seropositivity cut-offs. The multiplexing was done in line with the standard Luminex protocol for epitope mapping, ensuring consistency across wells and plates[16].

Epitope mapping

Antigen epitope mapping was conducted through x-MAP technology (Luminex Corp., USA) at ISGlobal to identify those epitopes exhibiting the highest IgG reactivity (measured by median fluorescence intensity, MFI) in convalescent serum samples. Initially, peptides were conjugated to X-MAP avidin magnetic beads via biotin conjugation with polyethylene glycol 12 (PEG-12), following the manufacturer's instructions (Luminex Corp.). Briefly, 1 mL of beads (1.25×10^6/mL) was sonicated for 20 s, washed and resuspended at 10,000 beads/ul in PBS-BSA 1%, followed by 20 s of vortexing and 20 s of sonication. Beads were washed thrice with PBS-BSA 1%, resuspended in freshly prepared 5 µg/1×10^6 beads of each peptide and incubated in a rotator for 30 min at room temperature, shielded from light. Subsequently, beads were washed thrice and resuspended at 10,000 beads/ul in PBS-BSA 1%. Finally, beads were stored protected from light at 4 °C until the commencement of the assay.

For the assay, serum samples were incubated with the multiplex at 4ºC overnight in agitation at 800 rpm. The following day, plates were washed and subsequently incubated with PE-Labeled anti-human IgG (MossBio, GTIG-001) for 30 min at room temperature with agitation at 800 rpm. Beads were washed and acquired using a FlexMap3D instrument. Statistical comparisons of MFI values across different groups were performed using the Mann–Whitney U test for independent sample comparisons, and one-way ANOVA followed by Bonferroni correction for multiple comparisons. These tests were selected due to their suitability for non-normally distributed and multiple-group data, respectively, and were applied using GraphPad Prism 9.3.0.

Each plate included a positive control curve, blanks controls, and 126 pre-pandemic samples as negative controls to determine the seropositivity cut-offs for each peptide[17]. Typically, home-made cut-off values are estimated using known independent negative sera, sometimes alongside positive ones, which are included in the titer plates amongst the unknown samples. A general formula for determining a cut-off value involves calculating the mean and standard deviation (SD) of independent negative control readings, (i.e., cut-off = mean + 3SD)[18,19]. In our study, cut-off values were defined following this approach, using the mean plus three standard deviations (mean + 3SD) of the MFI values obtained from 126 pre-pandemic negative control samples included in each plate.

The frequencies of positive samples (above the seropositivity cut-off) for each epitope, were utilized to evaluate the most immunogenic peptides. Multiplexing tests were carried out, and the MFIs between singleplex and multiplex assays were compared at various dilutions (1:50, 1:1000, 1:10000, 1:20000, 1:40000), demonstrating consistent MFI values across formats, confirming the reliability of multiplexing.

Production of monoclonal antibodies

mAbs were produced using Phage Display technology by ProteoGenix S.A.S (https://www.proteogenix.science/, Schiltigheim, FRANCE). The three selected epitopes, 3, 11 and 25 (synthesized as peptides < 20 AA with >95% purity, as required by Proteogenix S.A.S to scale up to antibodies production), were conjugated to BSA, OVA, KLH, and biotin carriers. A human immune scFv (single-chain variable fragment) library, LiAb-SFCOVID-19TM, derived from patients who recovered from COVID-19 (with a high diversity of $1.19 \times 10\text{^}10$ variants), was used for panning. Preliminary depletion against BSA, OVA, and KLH was performed before panning.

The elution of phage binders was performed using Glycine-HCl. The concentration of eluted phages (output pfu) was determined using E. coli TG1, which was also used for the amplification of the eluted phages.

ELISA immunoassays were conducted to screen for polyclonal (phage pools) and monoclonal phages (single phage binders) using an anti-phage-HRP antibody. ELISA plates were coated with either peptide conjugated to carriers or with the carriers alone. For monoclonal phages, single TG1 clones were randomly picked from plates and cultured with a helper phage followed by supernatant collection and screening. Positive single clones were then sequenced, followed by recombinant expression of the antibodies using ProteoGenix's proprietary XtenCHOTM cell line and purification on a ProteinA/G resin. The QC of recombinant antibodies was performed by Bradford assay using BGG standard (concentration determination), SDS-PAGE (purity and integrity assessment) and ELISA (functionality assessment).

Engineering framework for ScFv

The epitope binder scFv fragments were engineered onto human IgG heavy and light chain constant regions. The human framework used was based on standard therapeutic antibody formats, ensuring compatibility for downstream applications, including therapeutic and diagnostic purposes.

Monoclonal antibodies affinity and kinetic analysis with surface plasmon resonance biosensor

The determination of binding kinetics and affinity constants of monoclonal antibodies mAb11 (mAb11-G12 and mAb11-E1 clones) and mAb25 (mAb25-F9 and mAb25-H6 clones) for the peptide 11 (Pep11) and 25 (Pep25) was conducted using a Surface Plasmon Resonance (SPR) biosensor, enabling real-time monitoring of biomolecular interactions. A proprietary biosensor previously described was utilized, operating under wavelength interrogation[20]. Pep11 and Pep25 conjugated to BSA carrier protein (Pep11-BSA and Pep25-BSA) were employed. The conjugates were covalently immobilized on gold sensor chip surfaces, previously modified with carboxylic groups. Briefly, a mixed self-assembled monolayer (SAM) comprising 16-mercaptohexadecanoic acid (MHDA) and 11-mercapto 1-undecanol (MuOH) (MHDA/MUOH, 1:5 ratio) was formed on the surface as previously described[21].

Carboxyl groups were then activated via carbodiimide ester formation using a mixture of 1-ethyl-3-(3-dimethylaminopropyl) carbodiimide (EDC) and N-hydroxysulfosuccinimide ester (NHS) (0.2 M/0.05 M in MES buffer) to facilitate the covalent binding to the Lys groups of the BSA in the peptide conjugates (100 µg/mL in acetate buffer pH 4.5). A final step of blocking with ethanolamine (EA, 1 M) was performed to inactivate any remaining activated groups. The reaction was monitored in real-time within the biosensor to appropriately select optimal biofunctionalization conditions. The SARS-CoV-2 S protein (S1 subunit, 2019 nCOV, original variant) was directly immobilized following an analogous protocol (20 µg/mL in MES buffer pH 5). A control sensor chip consisting of a BSA biofunctionalized surface was prepared for control experiments employing the same conditions as described previously for the peptide conjugates ([BSA] = 20 µg/mL). MilliQ water was used as a running medium throughout the immobilization protocols.

The assessment of binding and association characteristics of each antibody for the Pep11 and Pep25 and the S1 protein was conducted in real-time. The running buffer was switched to PBS 10 mM pH 7.5 and successive injections of the antibody at various concentrations in PBS 10 mM (ranging from 6.6 to 264 nanomolar [nM] depending on the antibody) were performed. A constant flow rate of 20 µL/min was maintained throughout the measurements. Association and dissociation curves were generated for each concentration. The surfaces modified with peptides and protein were fully regenerated employing NaOH 25 mM injected at a flow rate of 30 µL/min to completely dissociate any remaining interactions. The real-time association curves were fitted to a binding-kinetics interaction model (Association and then Dissociation equation) using GraphPad Prism 9.3.0. This equation determines a comprehensive kinetic profile by globally fitting the data obtained with multiple analyte concentrations (nM) and analysing the sequential association (ka) and dissociation (kd) rates from the plot of ΔλSPR (nM) vs. time (min) of a minimum of four dose-responsive curves with their respective replicates. All the analyses assumed that binding follows the law of mass action, and the fitting method used was the Least Squares Regression. To provide a thorough analysis of the goodness of the fit, the adjusted R-squared was reported as an indicator of the fitting confidence, the Akaike's Information Criterion (AIC) value was reported for model validation, and the Sy.x value was reported for the dispersion measure of the residuals. A control surface with native BSA immobilized following a similar protocol was prepared to assess any potential nonspecific interactions of the antibodies with the protein, considering the highest concentration of Ab tested in each case (Figure S1 in Supplementary Information). The association and dissociation curves were fitted using the association-dissociation model equation via non-linear least squares regression (GraphPad Prism 9.3.0). Model performance was assessed using adjusted R^2, Akaike Information Criterion (AIC), and the standard deviation of residuals (Sy.x), ensuring robustness of parameter estimation.

Results

Characteristics of the participants with clinical-demographic data

Out of the 397 non-anonymous donors recruited at Hospital Clínic de Barcelona with clinical-demographical data, 198 were females and 199 were males. Additionally, 29 (7.3%) were asymptomatic, 181 (45.6%) presented mild symptoms, 70 (17.6%) moderate, and 117 (29.5%) severe. Of note, having fever, cough or/and dyspnoea was associated to COVID-19 severity. Clinical characteristics are presented in Table 1.

The significant p-values for IgG + and IgG+++ (both less than 0.001) underscore a notable positive association between IgG antibody levels and COVID-19 severity. The varying prevalence of IgG levels across severity groups suggests that the mid-term immune response (35 days), as reflected by SARS-CoV-2 antibodies, positively correlates with the severity of the condition.

Although Table 1 highlights the distribution of male and female participants, a more detailed stratified analysis of severity distribution by sex has been included. This analysis revealed that males exhibited a higher prevalence of severe cases compared to females, consistent with other COVID-19 studies showing sex-based differences in disease severity.

In silico refinement of the epitope landscape prediction in Spike protein of SARS-CoV-2

The B-cell epitope candidates refined in silico using Brewpitopes[9] targeted extra viral regions, non-glycosylated epitopes and regions accessible on the surface of SS protein (Fig. 2). These characteristics enhance their potential for recognition by neutralizing antibodies against SARS-CoV-2. Upon the refined predictions, to obtain a final list of consensus candidates we designed the Epixtractor and Epiconsensus[9]. These modules of Brewpitopes extract and integrate overlapping epitopes predicted using different tools into aggregated epitope regions. Then, these regions were ranked based on the following criteria among predictors: firstly, sorted by the best Bepipred v2.0 score[12]; secondly, arranged by the best Discotope v2.0 score[11]; and thirdly, ordered by the best ABCpred score[10]. As a result, we selected 25 linear B-cell epitopes with enhanced immunogenic potential which were included in a SARS-CoV-2 S Luminex panel for experimental validation[9].

In Fig. 2, we initially described the presence of 12, 8, and 5 epitopes in different regions of the S protein. Upon closer inspection, the figure now highlights the specific accessible epitopes on the trimeric structure of the S

	Overall	Asymptomatic 29 (6.65%)	Mild 181 (41.51%)	Moderate 70 (16.06%)	Severe 117 (26.83%)	*P*-value
Sex						
Female	198 (49.87%)	19 (9.6%)	113 (57.07%)	33 (16.67%)	33 (16.67%)	$<0.001^{ce}$
Lateral flow immunoassays						
Negative	67 (17.68%)	12 (17.91%)	44 (65.67%)	7 (10.45%)	4 (5.97%)	$<0.001^{bce}$
IgG+	63 (16.62%)	6 (9.52%)	39 (61.90%)	6 (9.52%)	12 (19.05%)	0.023^{de}
IgG++	77 (20.32%)	4 (5.19%)	36 (46.75%)	19 (24.68%)	18 (23.38%)	0.182
IgG+++	172 (45.38%)	7 (4.07%)	51 (29.65%)	33 (19.19%)	81 (47.09%)	$<0.001^{cde}$
Symptoms						
Fever	261 (65.74%)	–	108 (41.38%)	56 (21.46%)	97 (37.16%)	$<0.001^{de}$
General malaise	137 (34.51%)	–	61 (44.53%)	26 (18.98%)	50 (36.5%)	0.289
Arthromyalgia	130 (32.75%)	–	65 (50%)	30 (23.08%)	35 (26.92%)	0.195
Headache	119 (29.97%)	–	77 (64.71%)	21 (17.65%)	21 (17.65%)	$<0.001^{e}$
Anosmia	143 (36.02%)	–	91 (63.64%)	34 (23.78%)	18 (12.59%)	$<0.001^{ef}$
Ageusia	129 (32.49%)	–	78 (60.47%)	29 (22.48%)	22 (17.05%)	$<0.001^{ef}$
Asthenia	147 (37.03%)	–	88 (59.86%)	32 (21.77%)	27 (18.37%)	$<0.001^{ef}$
Gastrointestinal symptoms	122 (30.73%)	–	52 (42.62%)	33 (27.05%)	37 (30.33%)	0.019^{d}
Cough	224 (56.42%)	–	85 (37.95%)	51 (22.77%)	88 (39.29%)	$<0.001^{de}$
Dyspnoea	159 (40.05%)	–	39 (24.53%)	41 (25.79%)	79 (49.69%)	$<0.001^{de}$
Others	168 (42.32%)	–	82 (48.81%)	44 (26.19%)	42 (25%)	0.002^{f}
Treatment						
Symptomatic	266 (67.17%)	–	82 (30.83%)	68 (25.56%)	116 (43.61%)	$<0.001^{de}$
Antibiotics	158 (39.9%)	–	–	52 (32.91%)	106 (67.09%)	0.003^{f}
Antivirals	126 (31.82%)	–	.	26 (20.63%)	100 (79.37%)	$<0.001^{f}$
Immunomodulatory	140 (35.35%)	–	.	31 (22.14%)	109 (77.86%)	$<0.001^{f}$
Corticosteroids	99 (25%)	–	.	11 (11.11%)	88 (88.89%)	$<0.001^{f}$
Complications						
Pneumonia	113 (28.46%)	–	–	26 (23.01%)	87 (76.99%)	$<0.01^{f}$
Other	8 (2.02%)	–	–	2 (25%)	6 (75%)	0.712
≥ 2 complications	25 (6.3%)	–	–	3 (12%)	22 (88%)	0.009^{f}

Table 1. Clinical characteristics of the participants recruited at hospital clínic ($n = 397$). Data are presented as n (%). Categorical variables were compared via Chi-square test or Fisher's exact test, as appropriate. $^{a}p < 0{,}0.05$ asymptomatic vs. mild, $^{b}p < 0{,}05$ asymptomatic vs. moderate, $^{c}p < 0{,}05$ asymptomatic vs. severe, $^{d}p < 0{,}05$ mild vs. moderate, $^{e}p < 0{,}05$ mild vs. severe, $^{f}p < 0{,}05$ moderate vs. severe. IgG + stands for weak positive, IgG + + for positive, and IgG+++ for strong positive. "Other symptoms" included anorexia, rhinorrhoea, itching, chest pain, and skin, ear, nose, throat, ophthalmologic or neurologic disorders, whereas "other complications" included cryptogenic organizing pneumonia, necrotizing pneumonia, hospital-acquired pneumonia, ventilator-associated pneumonia, coagulopathies, and vascular or cardiological complications. Treatment of hospitalized patients was obtained from clinical history records. Lateral flow immunoassays were received after the recruitment period began, and hence data from 18 patients are missing (total sample size for this variable: $n = 379$).

protein, making it easier to visually distinguish these epitopes. The figure legend has been updated to ensure that the exact number of epitopes corresponding to each region is clearly identifiable.

Epitope screening by luminex

The 25 synthetized peptides were validated against 40 serum samples from convalescent COVID-19 patients, encompassing mild, moderate, and severe cases, thus representing the entire population, along with 126 pre-pandemic samples serving as negative controls for estimating seropositivity cut-offs. The 8 peptides (peptides 3, 10, 11, 15, 16, 24, 25, and 26) exhibiting the highest IgG reactivities were selected for the final screening against the 509 samples (Fig. 3).

The selection of 8 out of the 25 epitopes based on pre-screening of 40 patients is strongly associated with the inclusion of mild, moderate, and severe cases, representing the entire population, and the fact that 3 epitopes selected in the pre-screening of 40 patients correspond to the 3 epitopes chosen in the final screening of 509 patients.

Among the 8 peptides tested, peptides 25 and 11 exhibited the highest MFIs and the highest percentages of seropositive patients (39% and 33%), thus being selected as candidates for mAbs production. Peptide 25, identified as the most immunogenic against convalescent serum and plasma, demonstrated seropositivity values of 39.25% surpassing the 7723.85 cut-off value in the pre-pandemic samples. Peptide 11 emerged as the second

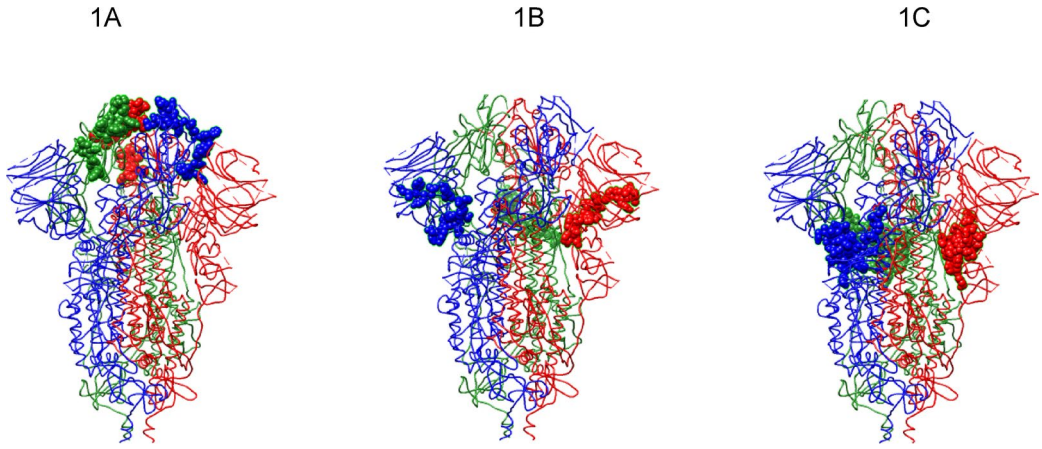

Fig. 2. Accessibility of candidate epitopes in the 3D conformation of the Spike protein. In silico analysis identified (**A**) 12 epitopes in the RBD domain, (**B**) 8 epitopes between both RBD and NTD domains, and (**C**) 5 epitopes in the NTD domain. Accessible epitopes are shown as sphered regions. Each chain of the Spike (S) protein trimeric structure is depicted in red, blue, and green backbones.

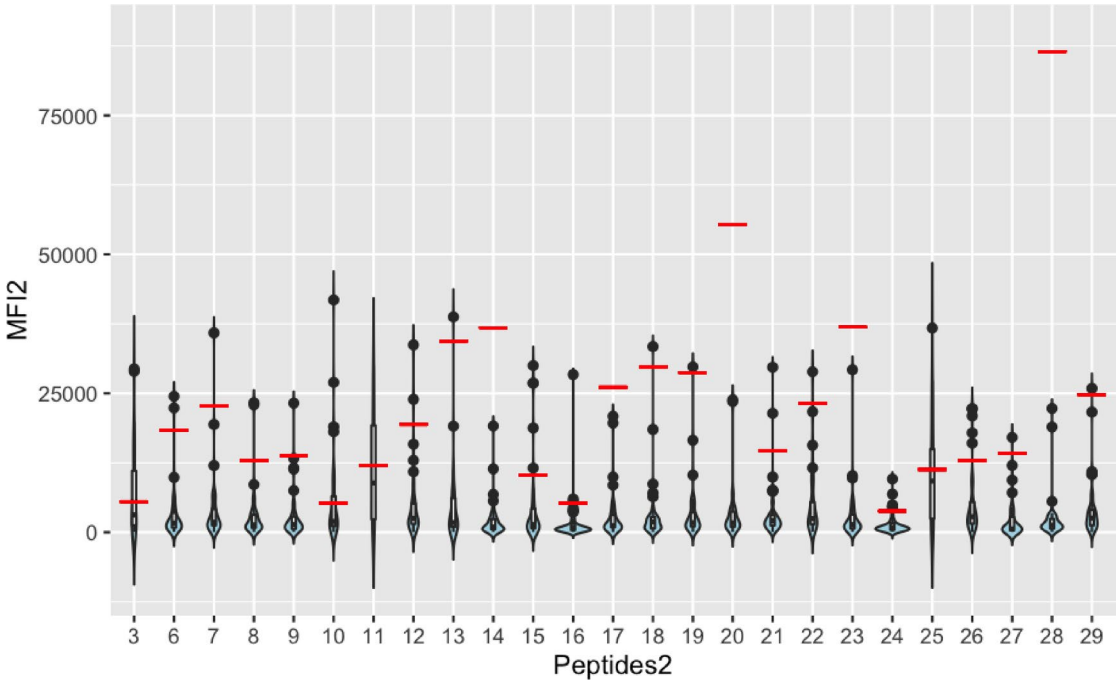

Fig. 3. IgG reactivity to the 25 synthetized peptides. IgG reactivity is depicted in violin plots; each plot represents one of the twenty-five peptides. Red lines indicate the seropositivity cut-off value for each peptide (mean + 3SD), and individual outliers are shown as dots.

best candidate, with a seropositivity rate of 33.13% starting from a MFIs cut-off of 10144.87. Intriguingly, both top candidates were located between RBD and NTD domains. Peptide 3 exhibited a seropositivity rate of 31.75% (above the 7002.30 MFIs cut-off), positioning it as the third best candidate. Peptides 10, 15, 16, 26, and 24 demonstrated lower percentages of seropositivity, as depicted in Fig. 4.

For Figs. 3 and 4, fluorescent signals from Luminex assays exhibited a lognormal distribution. To ensure accuracy in the cut-offs used, the MFI values were logarithmically transformed before analysis. This adjustment ensures that the calculation of 3SD cut-offs is meaningful and improves the robustness of the results.

Selection of peptides for monoclonal antibodies production

The selected peptides were not solely chosen based on the highest reactivity but on their ability to discriminate between seropositive and seronegative samples. The selection criterion emphasizes the discriminatory power of these peptides, aligning with their potential for mAb production and diagnostic purposes. The positions

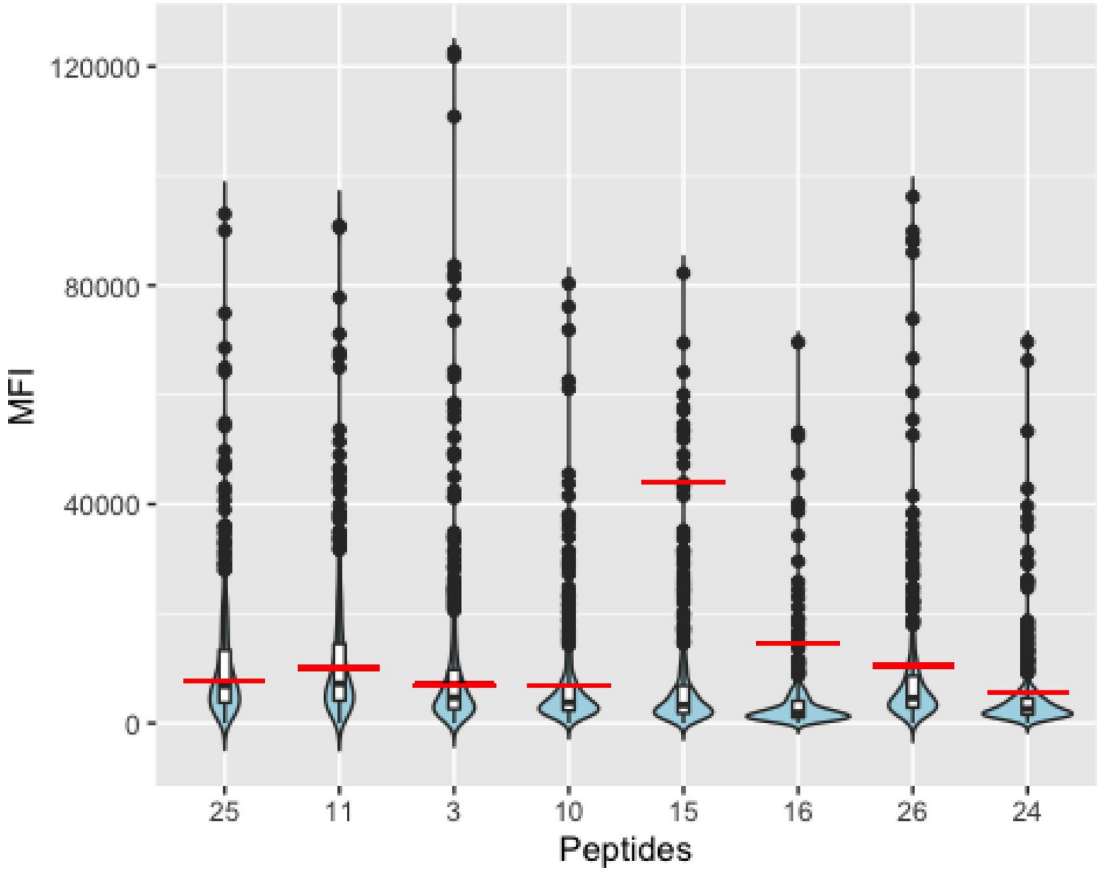

Fig. 4. IgG reactivity to the 8 selected peptides. Violin plots show IgG reactivity distribution for each of the eight peptides. Red lines indicate the seropositivity cut-off value for each peptide (mean + 3SD), and individual outliers are represented as dots.

and sequences of the selected and characterized epitopes are disclosed in the data availability section. This information includes the exact amino acid sequences of each epitope and their respective positions within the S protein. This transparency allows for a deeper understanding of the rationale behind the binding behavior observed in SPR experiments.

A phage display screening was conducted with the three best epitopes, using a phage library containing 10^9 anti-SARS-CoV-2 antibody clones to produce mAbs via phage technology at a private company. Two out of the three most immunogenic epitopes were scaled up, resulting in the generation of two monoclonal antibodies: mAb11 (mAb11-G12 and mAb11-E1 clones) and mAb25 (mAb25-F9 and mAb25-H6 clones), respectively.

Conservation analysis of selected epitopes

To further support the selection of the most immunogenic epitopes, we evaluated their conservation across the main SARS-CoV-2 VOCs. Using variant-specific S protein sequences reconstructed with mutations from the CoVariants/GISAID database, peptides 11 and 25 were mapped to assess their presence across Alpha, Beta, Gamma, Delta, and Omicron variants. Peptide 11 was fully conserved in all VOCs. Peptide 25 was conserved in all except the Delta variant, which contains a single amino acid change (T482K). This mutation introduces a positive charge that could impact antibody binding, although its C-terminal location may mitigate this effect. These findings confirm the high conservation of the selected epitopes and support their suitability as targets for antibody-based interventions. A summary of the alignment and conservation analysis is presented in Figure S2 in Supplementary Information.

Determination of binding affinities of the antibodies for the selected peptides

The affinity data and binding kinetics of the antibodies mAb11 and mAb25 for the Pep11 and Pep25, employed respectively as immunogens, were characterized through Surface Plasmon Resonance (SPR) label-free biosensing[22]. Peptide-based sensor chips were prepared, with peptides coupled to a carrier protein such as BSA (BSA conjugates) to facilitate attachment to the surface and enhance accessibility for the antibody-epitope interaction. This allowed the Lys groups in the protein to be available for covalent linkage to the surface previously modified with carboxyl groups[23]. Three different surfaces were biofunctionalized with Pep11-BSA, Pep25-BSA, and the S1 protein from SARS-CoV2 (as a reference) and each surface was evaluated with the antibodies: mAb11 (mAb11-G12 and mAb11-E1 clones), mAb25 (mAb25 -F9 and mAb25 -H6 clones), and a commercial antibody

(a neutralizing mAb targeting the RBD region). Injections of the antibodies over the different modified surfaces were conducted to generate real-time curves illustrating specific association and dissociation over time. The binding exhibited significant differences depending on the peptide-antibody interaction. The specific binding was initially confirmed by injecting the 4 mAb clones over a surface with only BSA, devoid of any specific epitope susceptible to recognition (either the Pep11, Pep25, or the S1 protein), resulting in negligible binding signals in all cases (data not shown). The results are summarized in Fig. 5, displaying fittings of the experimental sensorgrams to theoretical kinetic parameters and statistical parameters for all fitted curves.

From the fitting equations in Table 2, it is possible to extract the association (K_{ass}) and dissociation (K_{dis}) kinetic rate constants and determine the equilibrium dissociation constant (K_D) for the interaction of each antibody/ligand system. The model used for determining the constants was compared with other binding kinetics models using the AIC to ensure the quality of the fit, with AIC exceeding 99.99% in all cases, confirming the reliability of the model.

As observed, the equilibrium constants generally fall within the nM range, indicating high affinity for all four antibodies against the selected peptides in most instances. As expected, mAb11-E1 and mAb11-G12 exhibit notably higher affinity for Pep11 (3.38 and 2.16 nM) compared to Pep25, which displays K_D values 1 order of magnitude higher (33.4 nM and 11.3 nM, respectively), primarily due to slower dissociation kinetics. Additionally, mAb25-F9 and mAb25-H6 demonstrate higher affinity for Pep25 (2.86 nM and 1.05 nM) than for peptide Pep11 (67.4 nM and 112 nM, respectively), also attributed to slower dissociation. When compared with the commercial antibody (neutralizing antibody) targeting the RBD region, the affinity values fall within the same range. Notably, this antibody exhibits higher affinity for Pep11 than for Pep25 (two orders of magnitude difference, K_D=0.38 nM and 17.5 nM, respectively), corroborating the peptide's location closer to the RBD region compared to Pep25. These findings are presented in Table 2. Additionally, the affinity of mAb11-E1 and mAb11-G12 also differs from the other two antibodies regarding their affinity for commercial S protein (original variant), as their affinity is markedly higher (14.2 ad 6.49 nM) compared to mAb25-F9 and mAb25-H6 (200 nM and 34.5 nM).

K_D: equilibrium dissociation constant (nM); K_{ass}: association rate constant ($\times 10^6$ $M^{-1} \cdot s^{-1}$); K_{dis}: dissociation rate constant (s^{-1}); Adj. R^2: adjusted coefficient of determination; Sy.x: standard error of the regression. Kinetic parameters were obtained by globally fitting sensorgrams to the association–dissociation model using non-linear least squares regression (GraphPad Prism 9.3.0). Data for a commercial anti-RBD monoclonal antibody and for binding to the S1 protein were included as references for comparative purposes.

Discussion

In this study, we used serum samples from a large population of convalescent COVID-19 patients ($N = 509$) to identify immunogenic epitopes to produce novel therapeutic mAb cocktails or new vaccines against SARS-CoV-2. Among these, the two most promising candidates were validated, mAbs were produced and their affinity to S protein was comparable to that obtained with a commercialized mAb, in particular for one of them (mAb11). Our findings suggest that not only RBD domain epitopes can be immunogenic but also other domains serve as potential targets for developing mAbs. In this study, we have identified two epitopes outside the RBD domain as the most immunogenic. Overall, our epitope screening has proven its capability to yield immunogenic epitopes and could be leveraged for future drug discovery purposes beyond COVID-19.

Monoclonal antibodies were generated using Pep11 and Pep25. This decision was based: first, on the higher proportion of seroconverted COVID-19 against these peptides after epitope mapping using 509 serum samples from patients; and second, on the use of a phage library containing 10^9 anti-SARS-CoV-2 antibody clones before scaling up to mAbs production (Proteogenix). The two monoclonal antibodies mAb11 and mAb25 displayed good affinity not only towards the Pep11 and Pep25, used for their production, but also towards S1 protein. In particular, mAb11 exhibited similar affinity to that of a commercially available mAb. Among the antibody clones (mAb11-G12 and mAb11-E1; mAb25-F9 and mAb25-H6) the differences in affinity can be attributed to the structural features of each clone, particularly the CDR regions, which influence binding specificity and affinity for different epitopes (Table 2).

Among the 25 candidate epitopes tested in Fig. 3, eight exhibited IgG reactivity and successfully distinguished seropositive from seronegative individuals. This success rate is comparable to those reported by Polvere et al. and Stoddard et al. The observed IgG reactivity and seropositivity suggest an underlying immunogenicity of these candidate epitopes. However, the lack of IgG reactivity and seropositivity distinction does not exclude the possibility of antibody recognition by other immunoglobulin subtypes (e.g., IgA) present in the lung or gut, which are common sites of SARS-CoV-2 but are less prevalent in serum.

Furthermore, findings from the pilot test conducted on 40 patients (Fig. 3) led to the prioritization of 8 candidate epitopes for expanded screening in 509 patients (Fig. 4). The large-scale screening identified 3 epitopes (same as in the pilot) with the highest IgG reactivity and seropositivity discrimination. At this stage, the detection of SARS-CoV-2-reactive antibodies in 2 out of 3 selected epitopes at sufficient levels for monoclonal antibody (mAb) production demonstrates a pipeline success rate of 66%. Therefore, the objective of applying quality filters to immunogenic epitopes for antibody reactivity was achieved with a notable success rate among those tested for mAb production.

Two previous studies by Polvere et al.[24] and Caitlin I. Stoddard[25] employed similar strategies combining bioinformatic predictions and epitope mapping. The first study aimed at identifying binding signatures (epitopes of interest) using ELISA for epitope mapping. However, they targeted S, M, and N proteins of SARS-CoV-2 and tested the predicted peptides against samples from 24 convalescent COVID-19 patients, without distinguishing severity levels, along with 4 negative controls (pre-pandemic). In our study, we tested 509 samples, including different severity levels, against a multiplex panel of first 25 and then 8 S peptides, enhancing the dataset and statistical power, thus rendering it more robust. Interestingly, in Polvere et al. study, peptide 2 (identified by

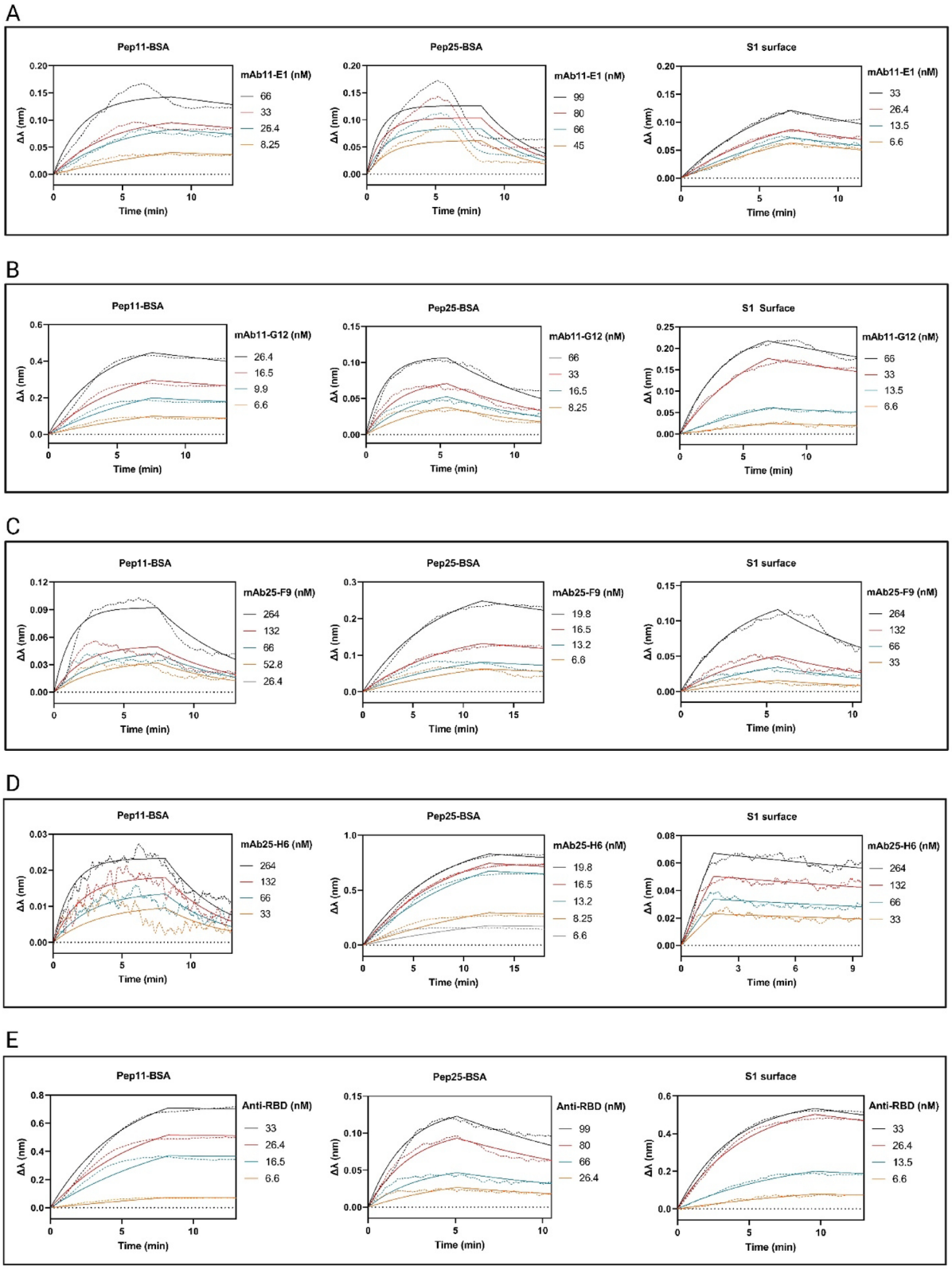

BepiPred v2.0) is homologous to our peptide 11[12]. However, in their study peptide 2 did not yield favorable results, differing from the results of our validation experiments. This discrepancy may be attributed to the smaller sample size of convalescent serum samples ($n = 24$) compared to ours ($n = 509$).

Additionally, we also identified the candidate epitope identified by them (our peptide 11). Yet, peptide 2 in Polvere et al.'s work consists of 30 amino acids (from 287 to 317), whilst our matching candidate (peptide 11) consists of 20 amino acids (from 280 to 300), making Polvere et al.'s epitope 10 amino acids longer. Additionally, their candidate terminates with a proline. Both, the longer extension and the Proline are not recommended for mAb production since they can lead to uncontrolled conformational changes, thereby reducing accessibility

◀**Fig. 5**. Surface Plasmon Resonance (SPR) binding analysis of monoclonal antibodies to different ligands. (**A**) E1 mAb11; (**B**) G12 mAb11; (**C**) F9 mAb25; (**D**) H6 mAab25; and (**E**) anti-RBD mAb (commercial neutralizing antibody targeting the RBD region). Peptides 11 and 25, as well as the S1 protein from SARS-CoV-2 (employed for comparison purposes), were covalently immobilized on the sensor chip surfaces as described in the *Methods* section. Overlayed sensorgrams (solid lines) and fitted curves (dotted lines) show the association and dissociation kinetics at different antibody concentrations. Association and dissociation rate constants, along with equilibrium dissociation constants, were extracted from the fitted equations in Table 2. Model fitting was evaluated using the Akaike Information Criterion (AIC), with values exceeding 99.99% in all cases, confirming the reliability of the kinetic model.

Antibody	Immobilized ligand	K_D (nM)	K_{ass} ($x10^6 s^{-1}$)	K_{dis} (s^{-1})	Adj. R^2	Sy.x
mAb11 mAb11-E1	Pep11-BSA	3.38	6.912	0.023	0.957	0.008
	Pep25-BSA	33.40	7.713	0.258	0.667	0.023
	S1 Protein	14.20	3.514	0.050	0.989	0.003
mAb11 mAb11-G12	Pep11-BSA	2.16	9.318	0.020	0.993	0.585
	Pep25-BSA	11.30	1.060	0.120	0.987	0.005
	S1 Protein	6.49	4.123	0.027	0.996	0.005
mAb25 mAb25-F9	Pep11-BSA	67.40	2.509	0.169	0.882	0.008
	Pep25-BSA	2.86	6.110	0.017	0.997	0.012
	S1 Protein	200.00	6.440	0.129	0.967	0.005
mAb25 mAb25-H6	Pep11-BSA	112.00	2.059	0.232	0.802	0.003
	Pep25-BSA	1.05	6.707	0.011	0.990	0.026
	S1 Protein	34.30	6.532	0.022	0.967	0.003
Commercial mAb (anti RBD)	Pep11-BSA	0.38	5.903	0.002	0.996	0.026
	Pep25-BSA	17.50	4.085	0.072	0.971	0.006
	S1 Protein	2.72	7.438	0.020	0.998	0.012

Table 2. *Kinetic and affinity parameters obtained from surface plasmon resonance (SPR) analysis of monoclonal antibodies binding to the peptides Pep11-BSA, Pep25-BSA, and the SARS-CoV-2 S1 protein.*

of the binding site[22]. They identified most of the epitopes of interest or binding sites on the S, N, and ORF1ab sequences. An advantage of the SARS-CoV-2 epitopes spanning positions 21 to 521 is their lack of cross-reactivity with other human coronaviruses, as demonstrated in this manuscript. This finding further validates our selected epitopes, as they are located in regions free from cross-reactivity with other human coronaviruses and remain unaltered in the Variants of Concern identified to date[26].

The second study akin to ours was conducted by Caitlin I. Stoddard et al.[25]. In this study, the authors identified binding signatures (epitopes of interest) and also explored their cross-reactivity with the 7 known human coronaviruses. However, their conclusions were based on the immune response observed in 19 serum samples from 19 COVID-19 patients (14 mild and 5 moderate/severe, without distinguishing between those hospitalized or requiring ICU admission), along with 5 negative controls (one of which was not definitively negative and could potentially be an asymptomatic COVID-19 case). Furthermore, they included 2 samples from SARS-CoV patients with unknown severity. They utilized a phage display library comprising the proteomes of the 7 human coronaviruses to map antibody binding sites (epitopes of interest) using the 26 serum samples to draw their conclusions.

Similarly to Polvere et al., Caitlin I. Stoddard et al. found most of the epitopes of interest on the S, N, and ORF1ab sequences. In comparison with the work of Caitlin I. Stoddard et al.[25], our approach is solely focused on SARS-CoV-2 rather than other human coronaviruses. In this regard, our strength lies in our cohort of 509 COVID-19 (asymptomatic, mild, moderate, and severe) samples, along with 126 negative controls, for Luminex epitope mapping, yielding more robust results. Their epitope comprises 38 amino acids from 281 to 319, which was not allocated in a region with cross-reaction but is terminated with a proline, as observed in the study by Polvere et al., which is not recommended as aforementioned[24].

Antibody levels at ICU admission are determinant for patients' ICU survival (ref: María Martin-Vicente et al., Journal of Internal Medicine, 2021). Long et al. (2020) suggested that severe COVID-19 patients tended to exhibit higher IgG antibody levels as detected by lateral flow immunoassay several days post-discharge, indicating a potential link between mid-term immune response strength and disease severity[27,28]. Our findings align with previous data also emphasizing the boost in immunity noticed in the most severe cases 35 days after hospital discharge.

The strengths of our work lie in the sample size of our cohort ($n = 509$) and the wide representation of different severity degrees, therefore ensuring the selected epitopes are not biased by COVID-19 severity[25]. However, the main limitation is the absence of modelling tools integrating artificial intelligence and molecular docking techniques, which has already opened new avenues for identifying potential immunogenic epitopes[29,30]. Nonetheless, it is crucial to acknowledge the variable precision and accuracy of these predictions, necessitating

careful validation of identified epitopes before downstream applications[29–33]. Moreover, it is important to acknowledge the dynamic nature of immune responses, as epitopes displaying robust reactivity during specific disease stages may not sustain the same level of immunogenicity over time[34]. Despite our mAbs displaying similar affinity with SARS-CoV-2 S1 S than commercially available mAbs, their in vivo neutralizing activity needs to be further investigated.

It is important to note that a direct correlation between SPR and Luminex data was not performed due to the fundamental differences between these two methodologies. Luminex quantifies polyclonal IgG reactivity in convalescent serum, providing a comprehensive overview of immune recognition, whereas SPR measures monoclonal antibody binding kinetics to individual epitopes under highly controlled conditions. By Luminex, epitopes 11 and 25 exhibited the highest seroreactivity, indicating strong immune recognition in polyclonal samples. By SPR the mAb11 and mAb25 yielded good recognition of the Pep11 and Pep25 used for their production and in particular mAb11 displayed comparable affinity to S1 protein than a commercially available mAb. Therefore, Luminex and SPR approaches were used in a complementary manner, providing a more comprehensive understanding of epitope immunogenicity and antibody binding properties.

In conclusion, while the identified epitopes and generated monoclonal antibodies have shown promise, further validation through in vivo neutralization assays is necessary. These assays will confirm the therapeutic potential of these mAbs in neutralizing SARS-CoV-2 and other potential variants. Further studies will focus on the neutralization efficacy and the potential for cross-reactivity with emerging variants of concern. The combination of bioinformatic methods to prioritize B-cell epitopes in silico via Brewpitopes with the use of convalescent serum for epitope mapping is a powerful pipeline for identifying potential therapeutic targets against SARS-CoV-2. Our two selected peptides (Pep11 and Pep25) were scaled up to mAb11 and mAb25 that recognise novel immunogenic regions of the S protein, distinct from the RBD domain and lacking cross-reactivity with other pre-existing coronaviruses, thereby facilitating further applications.

Data availability

All data generated or analysed during this study are available by contacting the corresponding authors.

Received: 14 January 2025; Accepted: 29 April 2025
Published online: 09 May 2025

References

1. Zhu, N. et al. A novel coronavirus from patients with pneumonia in China, 2019. *N Engl. J. Med.* **382**(8), 727–733 (2020).
2. Wang, C. et al. A human monoclonal antibody blocking SARS-CoV-2 infection. *Nat. Commun.* **11**(1), 2251 (2020).
3. McCallum, M. et al. N-terminal domain antigenic mapping reveals a site of vulnerability for SARS-CoV-2. *Cell* **184**(9), 2332–2347e16 (2021).
4. Pinto, D. et al. Cross-neutralization of SARS-CoV-2 by a human monoclonal SARS-CoV antibody. *Nature* **583**(7815), 290–295 (2020).
5. Ju, B. et al. Human neutralizing antibodies elicited by SARS-CoV-2 infection. *Nature* **584**(7819), 115–119 (2020).
6. Greaney, A. J. et al. Comprehensive mapping of mutations in the SARS-CoV-2 receptor-binding domain that affect recognition by polyclonal human plasma antibodies. *Cell. Host Microbe.* **29**(3), 463–476.e6 (2021).
7. Li, D. et al. The functions of SARS-CoV-2 neutralizing and infection-enhancing antibodies in vitro and in mice and nonhuman primates. *BioRxiv*. 2020.12.31.424729. (2021).
8. Andreano, E. et al. Extremely potent human monoclonal antibodies from COVID-19 convalescent patients. *Cell* **184**(7), 1821–1835.e16 (2021).
9. Farriol-Duran, R., López-Aladid, R., Porta-Pardo, E., Torres, A. & Fernández-Barat, L. Brewpitopes: a pipeline to refine B-cell epitope predictions during public health emergencies. *Front. Immunol.* **14**, 1278534 (2023).
10. Saha, S. & Raghava, G. P. S. Prediction of continuous B-cell epitopes in an antigen using recurrent neural network. *Proteins* **65**(1), 40–48 (2006).
11. Kringelum, J. V., Lundegaard, C., Lund, O., Nielsen, M. & Reliable, B. Cell epitope predictions: impacts of method development and improved benchmarking. *PLoS Comput. Biol.* **8**(12), e1002829 (2012).
12. Jespersen, M. C., Peters, B., Nielsen, M. & Marcatili, P. BepiPred-2.0: improving sequence-based B-cell epitope prediction using conformational epitopes. *Nucleic Acids Res.* **45**(W1), W24–W29 (2017).
13. Dobson, L., Reményi, I. & Tusnády, G. E. CCTOP: a consensus constrained topology prediction web server. *Nucleic Acids Res.* **43**(W1), W408–412 (2015).
14. Gupta, R. & Brunak, S. Prediction of glycosylation across the human proteome and the correlation to protein function. *Pac. Symp. Biocomput*. 310–322. (2002).
15. Steentoft, C. et al. Precision mapping of the human O-GalNAc glycoproteome through simplecell technology. *EMBO J.* **32**(10), 1478–1488 (2013).
16. Dobaño, C. et al. Highly sensitive and specific multiplex antibody assays to quantify immunoglobulins M, A, and G against SARS-CoV-2 antigens. *J. Clin. Microbiol.* **59**(2), e01731–e01720 (2021).
17. van der Wal, F. J. et al. Proof of concept for multiplex detection of antibodies against Chlamydia species in chicken serum using a bead-based suspension array with peptides as antigens. *Vet. Res.* **54**(1), 31 (2023).
18. Ridge, S. E. & Vizard, A. L. Determination of the optimal cutoff value for a serological assay: an example using the Johne's absorbed EIA. *J. Clin. Microbiol.* **31**(5), 1256–1261 (1993).
19. Jin, J. M. et al. Gender differences in patients with COVID-19: focus on severity and mortality. *Front. Public. Health.* **8**, 152 (2020).
20. Treviño, J., Calle, A., Rodríguez-Frade, J. M., Mellado, M. & Lechuga, L. M. Surface plasmon resonance immunoassay analysis of pituitary hormones in urine and serum samples. *Clin. Chim. Acta.* **403**(1–2), 56–62 (2009).
21. Lechuga, L. M. et al. Detection and quantification of HspX antigen in sputum samples using plasmonic biosensing: toward a real Point-of-Care (POC) for tuberculosis diagnosis. *ACS Infect. Dis.* **6**(5), 1110–1120 (2020).
22. Prada, Y. A. et al. Design and characterization of high-affinity synthetic peptides as bioreceptors for diagnosis of cutaneous leishmaniasis. *Anal. Bioanal Chem.* **413**(17), 4545–4555 (2021).
23. Calvo-Lozano, O. et al. Label-Free plasmonic biosensor for rapid, quantitative, and highly sensitive COVID-19 serology: implementation and clinical validation. *Anal. Chem.* **94**(2), 975–984 (2022).
24. Polvere, I. et al. A peptide-based assay discriminates individual antibody response to SARS-CoV-2. *Genes Dis.* **9**(1), 275–281 (2022).

25. Stoddard, C. I. et al. Epitope profiling reveals binding signatures of SARS-CoV-2 immune response in natural infection and cross-reactivity with endemic human CoVs. *Cell. Rep.* **35**(8), 109164 (2021).
26. Lv, H. et al. Cross-reactive antibody response between SARS-CoV-2 and SARS-CoV infections. *Cell. Rep.* **31**(9), 107725 (2020).
27. Long, Q. X. et al. Antibody responses to SARS-CoV-2 in patients with COVID-19. *Nat. Med.* **26**(6), 845–848 (2020).
28. Martin-Vicente, M. et al. Low anti-SARS-CoV-2 S antibody levels predict increased mortality and dissemination of viral components in the blood of critical COVID-19 patients. *J. Intern. Med.* **291**(2), 232–240 (2022).
29. Chatterjee, B., Singh Sandhu, H. & Dixit, N. M. Modeling recapitulates the heterogeneous outcomes of SARS-CoV-2 infection and quantifies the differences in the innate immune and CD8 T-cell responses between patients experiencing mild and severe symptoms. *PLoS Pathog.* **18**(6), e1010630 (2022).
30. Bukhari, S. N. H., Jain, A., Haq, E., Mehbodniya, A. & Webber, J. Machine learning techniques for the prediction of B-Cell and T-Cell epitopes as potential vaccine targets with a specific focus on SARS-CoV-2 pathogen: A review. *Pathogens* **11**(2), 146 (2022).
31. Grifoni, A. et al. Targets of T cell responses to SARS-CoV-2 coronavirus in humans with COVID-19 disease and unexposed individuals. *Cell* **181**(7), 1489–1501.e15 (2020).
32. Starr, T. N., Greaney, A. J., Dingens, A. S. & Bloom, J. D. Complete map of SARS-CoV-2 RBD mutations that escape the monoclonal antibody LY-CoV555 and its cocktail with LY-CoV016. *BioRxiv*. 2021.02.17.431683. (2021).
33. Fleri, W. et al. The immune epitope database and analysis resource in epitope discovery and synthetic vaccine design. *Front. Immunol.* **8**, 278 (2017).
34. Titov, A. et al. Immunogenic epitope panel for accurate detection of non-cross-reactive T cell response to SARS-CoV-2. *JCI Insight*. **7**(9), e157699 (2022).

Acknowledgements

We are indebted to the nursing staff at Hospital Clínic and to the patients for their generous donations. We also acknowledge Fundació Glòria Soler for supporting the COVIDBANK initiative and the HCB-IDIBAPS Biobank for providing biological human samples and data. Additionally, we acknowledge the contributions of Marcelo Viegas and Mathieu Schaff from ProteoGenix S.A.S for their invaluable technical support during mAb development.

Author contributions

RLA, LBF, RF, and LFB contributed to the study's design, data analysis, and manuscript writing. LFB and AT secured funding, while LFB oversaw reporting and served as the principal investigator for the research. RLA and LFB designed the study protocol and established the research consortium. RLA and RF conducted the computational analyses and integrated bioinformatics tools into the pipeline. All authors participated in the clinical management of patients and/or contributed to data and sample collection and processing. RA, MV, AJ, GM, AGB, and CD performed epitope screening using Luminex. MDP, MCE, and LL designed and conducted the kinetic and affinity studies using SPR. All authors contributed to the critical review of the manuscript. Additionally, RLA, LBF, RF, and LFB were responsible for drafting and revising the manuscript throughout the review process.

Funding

GENCAT-DGRIS- COVID19, to AT/LFB. CB 06/06/0028/CIBER de Enfermedades Respiratorias – CIBERES ISCIII-FEDER-FSE (FI19/00090 awarded to RLA). ICREA Academy / Institució Catalana de Recerca i Estudis Avançats to AT, 2.603 / IDIBAPS, SGR/Generalitat de Catalunya to AT and LFB. Funders did not play any role in the study design, data collection, data analysis, interpretation, or the writing of the manuscript. ICN2 is funded by the CERCA programme (Generalitat de Catalunya). The ICN2 is supported by Severo Ochoa Centres of Excellence programme, Grant CEX2021-001214-S, funded by MCIN/AEI/10.13039.501100011033. The NanoB2A group is a consolidated research group (Grup de Recerca) of the Generalitat de Catalunya and has support from the Departament de Recerca i Universitats de la Generalitat de Catalunya (expedient: 2021 SGR 00456). The NanoB2A group acknowledges financial support from the European Commission – NextGenerationEU (Regulation EU 2020/2094), through CSIC's Global Health Platform (PTI Salud Global – Iniciativa Estratégica de Diagnóstico).

Declarations

Consent for publication

I, the undersigned, give my consent for the publication of identifiable details, which can include Figure(s) and/or data and/or details within the text ("Material") to be published in the above Journal and Article.

Ethics approval and consent to participate

HCB/2020/0332.

Competing interests

The authors declare no competing interests.

Additional information

Supplementary Information The online version contains supplementary material available at https://doi.org/10.1038/s41598-025-00555-9.

Correspondence and requests for materials should be addressed to R.L.-A., A.T. or L.F.-B.